Journal of Applied Electrochemistry (2020) 50:689–697
https://doi.org/10.1007/s10800-020-01423-2

RESEARCH ARTICLE

Additive manufacturing of monolithic supercapacitors with biopolymer separator

Maedeh Arvani[1,2] · Jari Keskinen[1] · Anna Railanmaa[1] · Sanna Siljander[3] · Tomas Björkqvist[3] · Sampo Tuukkanen[4] · Donald Lupo[1]

Received: 17 October 2019 / Accepted: 7 April 2020 / Published online: 2 May 2020

Abstract

In this paper, additive layer-by-layer fabrication of a fully screen printed monolithic supercapacitor exhibiting performance comparable with supercapacitors prepared using lamination is reported. A novel separator material improves the performance of the monolithic supercapacitor, is easily applicable using scalable processes such as screen and stencil printing, and is based on sustainable biomaterials. The additive monolithic manufacturing offers advantages for system integration and avoids the need of an additional alignment step as needed in the fabrication of laminated supercapacitors. Previously, the monolithically fabricated supercapacitors showed higher equivalent series resistance (ESR) and leakage current than the laminated ones. By using microfibrillated cellulose (MFC) and chitosan as separator materials ESR and leakage current were decreased. These disposable and non-toxic aqueous electrolyte supercapacitors are optimized for autonomous sensor systems, for example in Internet-of-Things (IoT) applications, with capacitance of 200–300 mF and ESR of about 10 Ω. The new composite separator material consisting of MFC and chitosan has good adhesion on the electrodes and the substrate, is easy to apply using printing and coating processes, and does not diffuse into the porous electrode.

Electronic supplementary material The online version of this article (https://doi.org/10.1007/s10800-020-01423-2) contains supplementary material, which is available to authorized users.

✉ Maedeh Arvani
arvanimaedeh@gmail.com

[1] Faculty of Electrical Engineering, Tampere University, Korkeakoulunkatu 7, 33720 Tampere, Finland

[2] Department of Physics, Åbo Akademi University, Porthansgatan 3, 20500 Turku, Finland

[3] Faculty of Automation Technology and Mechanical Engineering, Tampere University, Korkeakoulunkatu 7, 33720 Tampere, Finland

[4] Faculty of Medicine and Health Technology, Tampere University, Korkeakoulunkatu 7, 33720 Tampere, Finland

Graphic Abstract

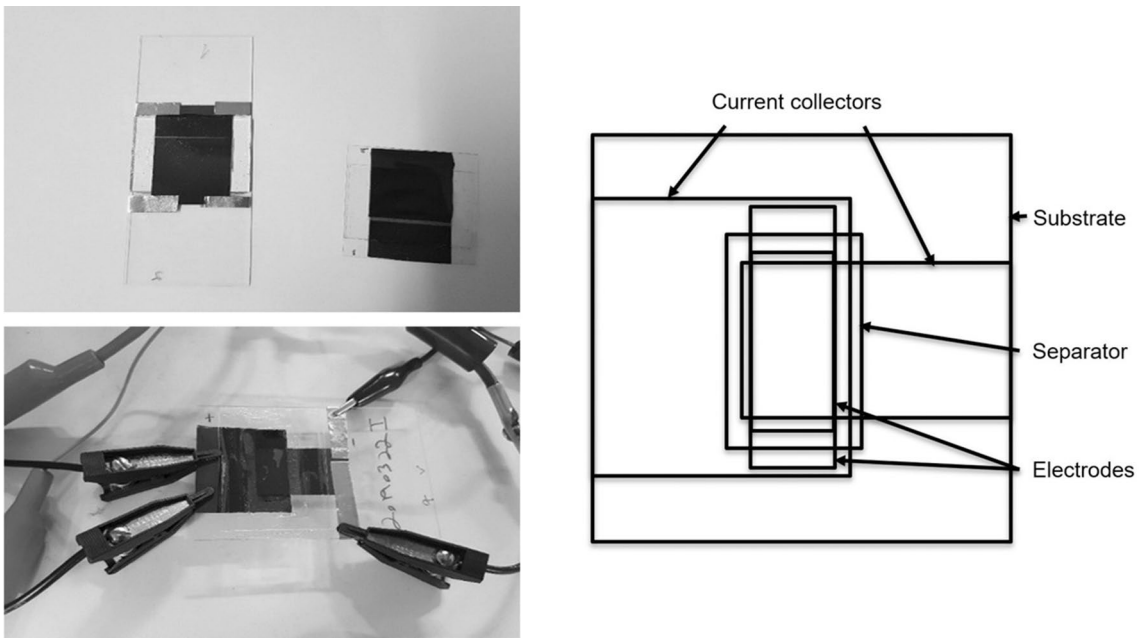

Keywords Supercapacitors · Energy storage · Printed electronics · Nanocellulose · Microfibrillated cellulose · MFC · Chitosan · Separator

1 Introduction

In the near future, it is expected that there will be billions [1] of devices which should all integrate and connect smoothly with the "Internet of Things" (IoT) in different services, for example smart homes, healthcare and industry automation. IoT devices and sensor networks need non-toxic and inexpensive ways to store energy [1, 2]. Supercapacitors [3–5] are in many cases a better choice than batteries for managing the energy storage due to their safety, disposability and higher cycle life [6].

Supercapacitors store energy into the electrochemical double-layer at a highly porous electrode surface. The key elements of a supercapacitor are current collectors, electrodes, separator and electrolyte. Printed supercapacitors are usually manufactured by applying two electrodes on the current collectors separately, laminating the electrodes face-to-face while sandwiching the separator between them and applying the electrolyte before encapsulation [7–10].

We report here the monolithic fabrication of supercapacitors, by applying the films layer by layer on top of each other on the substrate. Monolithic fabrication can have advantages over the conventional lamination approach, both for system integration and for fabrication of series connected modules when higher voltage is needed. Previously reported monolithically fabricated aqueous supercapacitors showed higher equivalent series resistance (ESR) and higher leakage current to capacitance ratio than laminated ones [11]. We have improved the performance by using a novel, bio-derived composite material as a separator, consisting of microfibrillated cellulose (MFC), also known as nanocellulose, and the polysaccharide chitosan.

The use of MFC in supercapacitors has been reported previously. However, most of these reports are concerned with the use of MFC-based conductive materials for electrodes and current collectors [12–15]. Other reports on MFC materials do not describe their application in supercapacitors but instead report the chemical properties of the material [16]. MFC-based cellulose papers have also been used as separators in supercapacitors [17], but these devices were assembled using lamination. A monolithically fabricated supercapacitor has also been reported previously [18], although the size and the materials of the supercapacitors were different from the ones reported here.

The separator of the supercapacitors must be thin and electrochemically stable. It must have high ionic conductivity [19]. On the other hand, the separator must prevent short circuit between the electrodes [4, 20]. The use of MFC as a separator material was previously reported by Tuukkanen et al. [21]. This work is motivated by the previous work and extends it to easier and more consistent

manufacturing and performance by forming a composite with the biopolymer chitosan.

2 Experimental methodology

2.1 Materials

Devices were prepared on both 1 mm thick Corning ® 2947 glass, and on polyethylene terephthalate (PET film, Melinex ST506 from DuPont Teijin Films, thickness 125 µm). The reason to use both rigid glass and flexible PET was to test whether flexibility causes any differences in the supercapacitor properties and to investigate the effect of different surface energies on adhesion of the formulations.

Graphite ink Acheson PF407C was used as current collector. The printed current collector layer was cured at 95 °C for 1 h. The electrodes were made from activated carbon (AC) Kuraray YP-80F, using chitosan (Sigma-Aldrich, 50494) as a binder using the formulation reported previously [7].

Chitosan, MFC and combinations of chitosan and MFC were compared as the separator materials, using cellulose paper (Dreamweaver Silver AR40 thickness 40 µm) as a control. The chitosan solution was made by mixing 2.7 g chitosan powder (Sigma-Aldrich, 50494), 67 g water and 0.7 g acetic acid. For dispersing of chitosan, acidic solution is required [22].

For preparation of MFC, Nordic bleached hardwood kraft pulp was refined in a low consistency (LC) refiner. The refined cellulose pulp was then fractionated. The fine fraction (accept fraction) was dewatered and stored in refrigerator at 25% consistency, whereas the reject fraction was not used in this study. The fine fraction containing 40% of fines (Bauer McNett Fiber Classifier-200) [23] was used as raw material for microfibrillation without any biocides added.

The fibrillation was performed with an in-house built mechanical laboratory scale fibrillator. The construction is a disc refiner type containing rotor and stator plates. Both plates have 110 mm outer diameter with fibrillation surfaces overall roughness in micrometer scale. The cellulose fiber slurry brought into the gap between the plates is exposed to mechanical shear and centrifugal forces which result in opening the fibril structures.

For the fibrillation stages, the pulp was diluted to 2.9% consistency. The rotation speed of the rotor was 4149 rpm, and the axial closing force of the plate gap was adjusted to keep the feeding pressure at 4 bar. The plate gap was gradually reduced at each stage by lowering the feeding rate. The three first stages were kept partly as homogenization of the cellulose slurry, because mixing in the feeding tank remained incomplete and relatively little energy was applied to the fibrillating process. The succeeding three stages changed the pulp from the slurry to an opaque gel-like substance. The last fibrillation stage was run with 150 ml/min feeding rate, which serves as a measure of fibrillation state.

All manufactured supercapacitors are environmentally friendly as the current collectors are made from graphite and the activated carbon used for the electrodes is made from coconut shell (information from the manufacturer). The separators are of paper, MFC or chitosan, which is made from shrimp shells. The electrolyte was diluted NaCl (Fluka 38979) to deionized water to obtain 1 M solution. Adhesive tape (468MP-200MP from 3 M) was used for sealing the supercapacitors.

2.2 Manufacturing

Screen printing was used to make the supercapacitor electrodes, due to its suitability as a low-cost, high-throughput process for depositing uniform thick films [24–27]. The only film that was not screen printed is the separator, which was deposited by stencil printing (doctor blade applicator using mtv Messtechnik Film Applicator) due to the low solid loading of the formulation, which is a typical property of nanostructur cellulosic materials. Alternatively, current collectors were also fabricated by stencil printing, which gave comparable results.

The cross section and layout of the supercapacitors are shown in Fig. 1. The cross section of a monolithic supercapacitor is shown schematically in the Fig. 1a, while the Fig. 1b presents the schematic cross section of a face-to-face laminated supercapacitor. Figure 1c presents the layout of the monolithic and laminated supercapacitors, which are the same.

The width and the length of the supercapacitors' substrates are 50 mm. The laminated supercapacitors are fabricated by applying the first 34 mm wide layer of the graphite ink as a current collector on the substrate. The next layer is 31 mm wide activated carbon as electrode. This sequence of electrodes is deposited onto two substrates. A paper separator is deposited onto one of the substrates, the two substrates are laminated together, and the device is filled with electrolyte before sealing with adhesive tape.

For the monolithic devices, the current collector and activated carbon electrode are deposited in the same way as the first two layers of the laminated device. The next layer is a 26 mm by 16 mm separator that can be of paper (physical placement) or from solution (blade coating). The upper layer of activated carbon (22 mm wide) and graphite ink (18 mm wide) are printed on top of the separator, and the device is sealed (the curved line in Fig. 1a) after electrolyte filling.

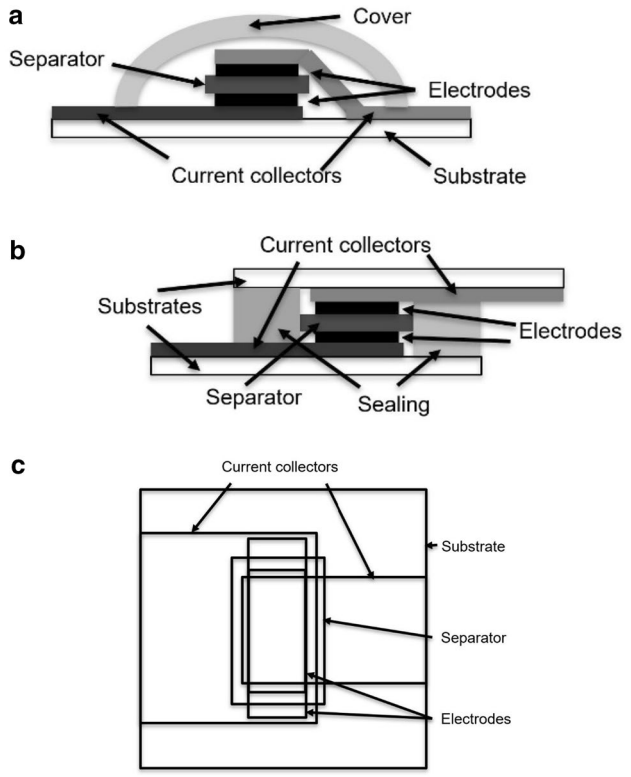

Fig. 1 Schematic cross section and layout of the monolithic supercapacitor (**a**) and the laminated supercapacitor (**b**) and the layout of both the monolithic supercapacitor and the laminated supercapacitor (**c**)

2.3 Characterization

The ionic conductivity across the separator layer was assessed with impedance spectroscopy [3, 28]. Measurements were done with a Zahner Zennium potentiostat in upper limit sweep mode: the measurement was initiated at 1 Hz with a frequency sweep up to 1 MHz and back down to 50 mHz. Voltage amplitude was 10 mV. Nyquist plots were obtained for each separator type and the ionic resistance R was estimated from the intersection of the curve and the x-axis, i.e. the real part Z' of the complex impedance. Ionic conductivity σ was then calculated using Eq. 1*:*

$$\sigma = \frac{l}{RA}, \tag{1}$$

where l is the separation between the electrodes and A is the surface area of one electrode. Each of the studied materials was prepared first as a dry sheet on a carrier substrate (Dreamweaver separator was used as is), from which they were peeled off, cut to the sample size of 9 cm^2 and soaked through with 1 M aqueous sodium chloride solution. The sample was then placed between two polished stainless steel electrodes and the thickness of the sample was obtained with a micrometer by measuring the thickness of the electrode plates with and without the separator in between.

The capacitance, ESR and leakage current were measured using a Maccor 4300 Electrochemical Test System, according to the IEC 62391-1 standard [29]. During the measurement procedure, the supercapacitors were charged and discharged with constant current (1, 3 and 10 mA) between 0 and 1.2 V three times. Then for 30 min, the voltage was held at 1.2 V. Subsequently, the capacitance was defined during the constant current discharge step between 0.96 and 0.48 V. The supercapacitors were then kept at constant voltage of 1.2 V [30]; the leakage current reported is the current required to maintain the voltage after 1 h. The process has been done for all discharge currents of 1, 3 and 10 mA; ESR is calculated from the IR drop in the measurement of 10 mA discharge current.

Scanning electron microscopy (SEM) using Zeiss Ultra-Plus FE-SEM with a 5 kV acceleration voltage was used for characterization of electrode and separator materials.

3 Results and discussion

3.1 Quality of the films

The MFC, chitosan, and combinations of these two materials in different ratios were used to make the separator film on activated carbon electrodes, PET and glass. Due to the layout of the monolithic supercapacitor, the separator should adhere well to all these materials to prevent a short circuit. Figure 2 shows the results. As we

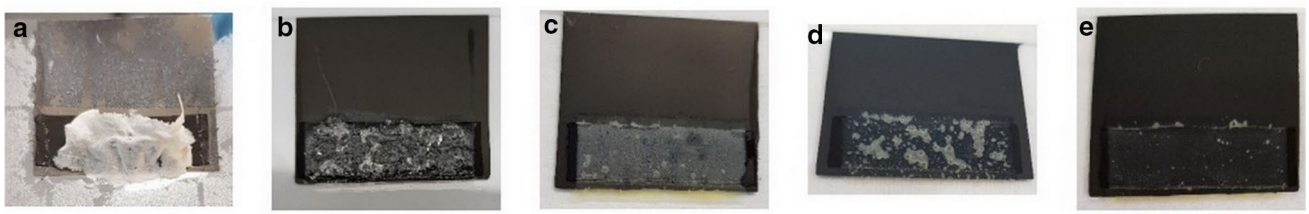

Fig. 2 **a** MFC, **b** Chitosan, **c** 80% MFC solution + 20% chitosan solution, **d** 80% Chitosan solution + 20%MFC solution, **e** 50% Chitosan solution + 50% MFC solution film on glass substrate

can see in Fig. 2a, during the drying step the pure MFC film is peeled off from the glass substrate, as there is poor adhesion between the underlying materials and the applied film. Chitosan (Fig. 2b) can cover the substrate and form the film but bubbles are easily formed when applying the chitosan solution with stencil printing. This is believed to be due to penetration of chitosan inside the activated carbon film, thus forcing air to come out from the pores of the activated carbon layer. These bubbles may cause a short circuit when the film is used as a separator. Figure 2c shows a film containing 80% MFC solution and 20% chitosan solution, which did not completely cover the substrate properly, leaving holes in the films. Figure 2d shows a film containing 80% chitosan solution and 20% MFC solution that still shows a bubbles, although a reduced. Figure 2e shows a film made of 50 wt% chitosan solution and 50 wt% MFC solution (CM5050). There are almost no bubbles and it covers the substrate uniformly. The chitosan in the formulation with weight ratio 20% MFC + 80% chitosan penetrates into the activated carbon, resulting in bubble generation when the air in the electrode is replaced with the solution, as was also observed with the pure chitosan film. A film with many bubbles is not a suitable separator; when the upper electrode is applied onto the separator, there exists considerable risk of short-circuit between the electrodes. The solution with weight ratio of 80% MFC solution + 20% chitosan does not form a closed film, thus does not cover the lower electrode well enough; this also increases the risk of short circuit. Thus these formulations were clearly not suitable and therefore not analysed further. Application of the CM5050 formulation was a simple one-step process and produced films of good quality and with good adhesion. Chitosan appears to act as both a binder and an adhesion promoter for MFC, which eliminates the peeling seen with pure MFC. Use of chitosan as both in electrode binder and composite separator may help improve adhesion and increase the film quality, enhancing the formation of homogeneous films.

3.2 Ionic resistance of the separators

The ionic resistances of the Dreamweaver paper, MFC, chitosan and CM5050 impregnated with 1 M NaCl are presented in Table 1.

The MFC separator shows the highest ionic conductivity, whereas paper and chitosan showed relatively lower values. The CM5050 separators shows almost as high conductivity as pure MFC, which makes it potentially a good choice for separator of supercapacitors, due to the easier film deposition.

Table 1 Thickness and ionic resistance values of the separators

Material	Thickness (μm)	Ionic resistance (Ωm)	Ionic conductivity (S/m)
Dreamweaver paper	95	3.4	0.3
MFC	150	1.0	1.0
Chitosan	159	2.6	0.38
CM5050	106	1.1	0.9

3.3 Microstructure

Figure 3 shows SEM images of the activated carbon, Dreamweaver paper, MFC, chitosan and CM5050. The AC surface is porous as expected. The fiber structure in MFC and CM5050 is obvious.

SEM images show particle size of about 1–10 μm and irregular shape of the activated carbon powder. The pores typical for activated carbon microstructure are not visible with this low magnification. In the supplementary material, micrographs with higher magnification are presented in Fig. S2. The Dreamweaver paper consists of fibers having different diameters, from about 100 nm to 1 μm. The images show the diameter of the fibers in MFC and CM5050 are 100 nm to 0.5 μm. When compared with Dreamweaver, MFC has a larger amount of smaller fibers. The bubbles on chitosan surface are obvious in the SEM image, while CM5050 shows almost no bubbles.

3.4 Electrical performance of the supercapacitors

The supercapacitor types fabricated in this study are listed in Table 2. Figure 4 shows the supercapacitors on glass and PET. Figure 4b shows an example of a supercapacitor on glass substrate connected for measurement. The results are reported in Table 2. The supercapacitors made using a pure MFC sheet did not work due to poor adhesion of the MFC film.

Supercapacitors A and B are face-to-face assembled references that were manufactured using the lamination method with Dreamweaver as a separator. The substrate of A is PET and the substrate of B is glass. The material and geometry of the supercapacitor C and D are the same as used in A and B, respectively, but C and D have the monolithic structure, in which the paper separator was manually deposited and the final layers were printed on top of it. C and D have higher ESR and higher specific leakage current than A and B. The increased ESR in the monolithic devices appears to be due to the formation of a high resistance edge upon printing the top layer or graphite as a current collector over the separator.

Supercapacitors E, F, G and H with chitosan or CM5050 separators show lower ESR and slightly higher leakage

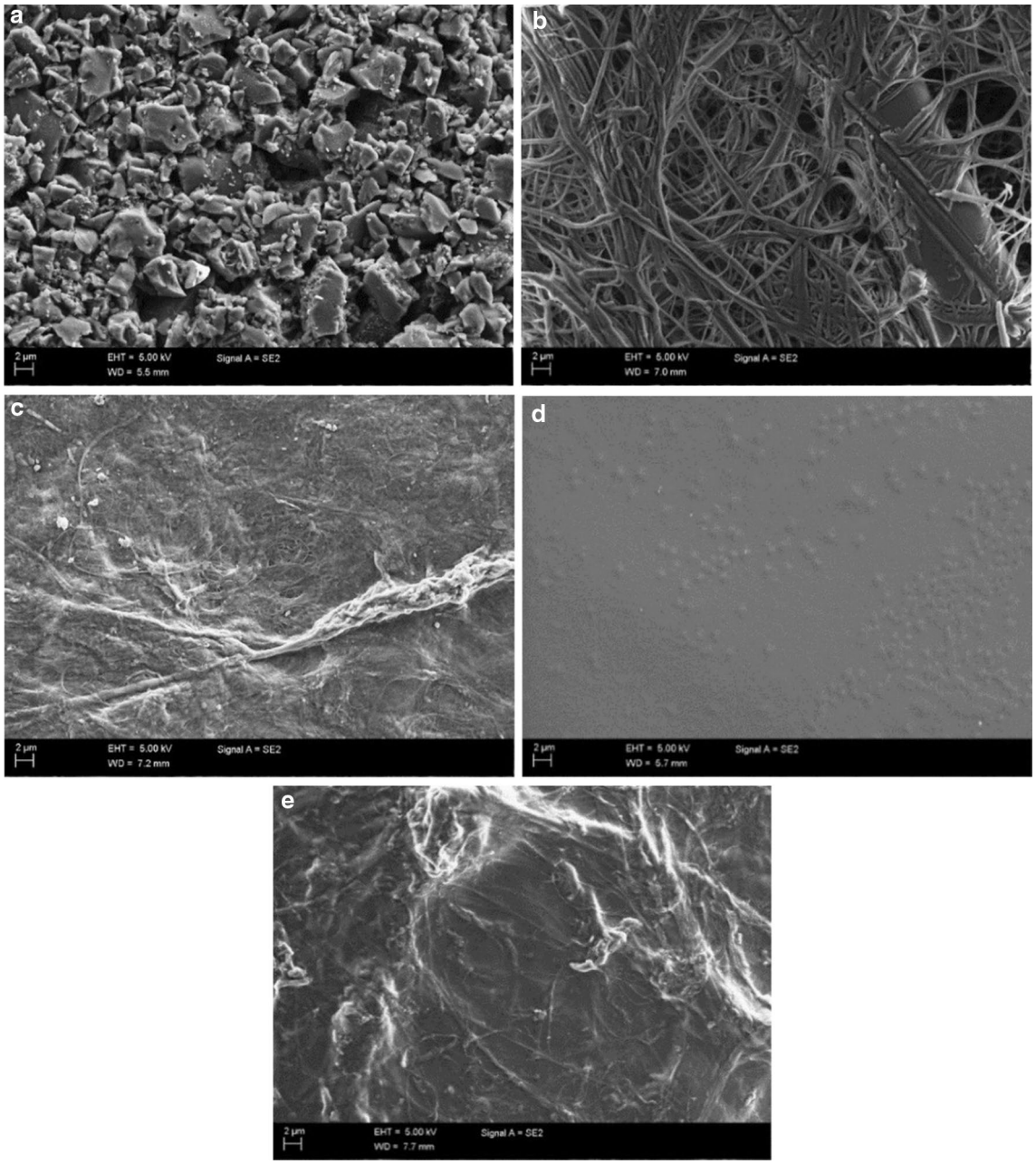

Fig. 3 SEM imaging of **a** Activated carbon, **b** Dreamweaver paper, **c** MFC, **d** Chitosan, **e** CM5050 (50 wt%Chitosan + 50 wt% MFC)

current relative to capacitance. Due to the comparative ease in depositing the CM5050 separator, it was used for further experiments, where the current collectors and electrodes are screen printed (type I in Table 2). The result is comparable with the supercapacitor G that is made by combined screen-printing (lower electrode) and stencil coating (upper electrode and current collectors). The numerical values presented in Table 2 for supercapacitors F, G and I are the averages of several devices. Detailed values are available in Supplementary material, Table S1.

Figure 5 shows the leakage current of the monolithic supercapacitors as a function of capacitance. Although the geometrical areas of the electrodes are the same, there is some variation in the thickness of the electrodes due to slight variations in the screen and stencil printing runs. In principle, the thicker the electrode is, the larger capacitance is obtained. The data agree with previous measurements [7] and show an increase in leakage current with capacitance. In supercapacitors, as leakage current is largely caused by Faradaic charge-transfer reactions at the electrodes. Thus

Table 2 Electrical properties of the supercapacitors

	Supercapacitor, architectural structure, substrate, separator	Capacitance (mF)	ESR (Ω)	Leakage current (μA)	Specific leakage current (μAF^{-1})
A	Reference, laminated, PET, paper	297	10.1	6.5	21
B	Reference, laminated, glass, paper	243	13.5	6.1	25
C	Monolithic, PET, paper	186	20.6	6.5	34
D	Monolithic, glass, paper	209	29	6.7	32
E	Monolithic, PET, chitosan	259	15.8	7.3	28
F	Monolithic, glass, chitosan	281	19.6	7.2	25
G	Monolithic, PET, CM5050	269	14.9	6.9	26
H	Monolithic, glass, CM5050	278	12.2	7.9	28
I	Monolithic, PET, CM5050 Current collectors and electrodes screen printed	315	12.7	8.1	26

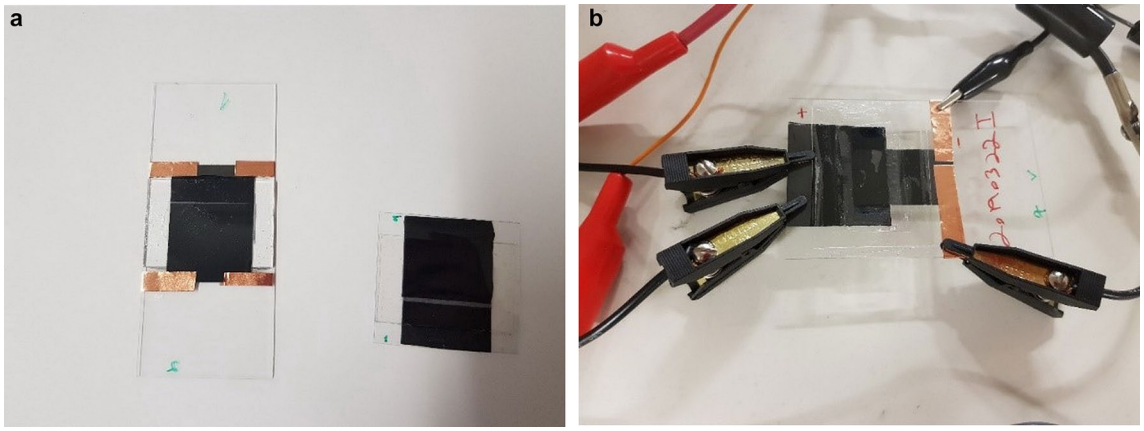

Fig. 4 **a** The monolithic supercapacitors on glass (left) and PET (right). **b** Monolithic supercapacitor connected with crocodile clips during measurement

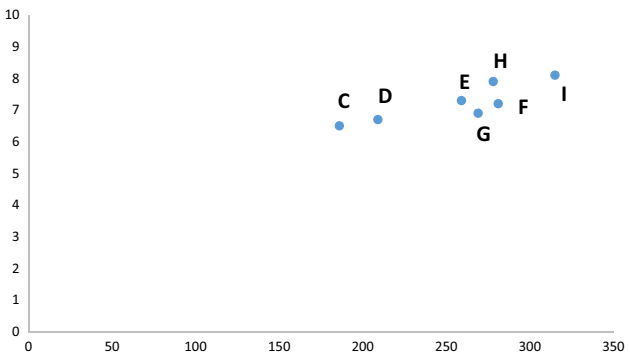

Fig. 5 Leakage current of the monolithic supercapacitors (C, D, E, F, G, H and I) as a function of capacitance

increasing the electrode surface area results in larger leakage current [7].

Figure 6 shows the galvanostatic charge and discharge of supercapacitor I at constant current 1 mA (Fig. 6a) and 10 mA (Fig. 6b).The IR drop is clearly observable. The galvanostatic charge–discharge curves of the other supercapacitors are provided in the Supplementary material, Fig. S1.

Compared to the other reported monolithic supercapacitors, both with aqueous [11] and ionic liquid electrolyte [18], our supercapacitors show considerably lower leakage current at comparable capacitance for the voltage of 1.2 V. The supercapacitor mentioned in reference [18] had ionic liquid electrolyte in gel-polymer and a polymer containing fluorine was used to bind the electrodes.

Tuukkanen et al. have reported the use of MFC in a laminated device [21]. Nanocellulose gel is applied by pipetting on to both electrodes and laminating. In our case, the supercapacitor is prepared monolithically and the separator is deposited by bar coating, which enables a fully printable monolithic supercapacitor. In the present work, we take the advantage of making a mixture of MFC and chitosan, to obtain better printability of separator layer and improve the mechanical and adhesion properties.

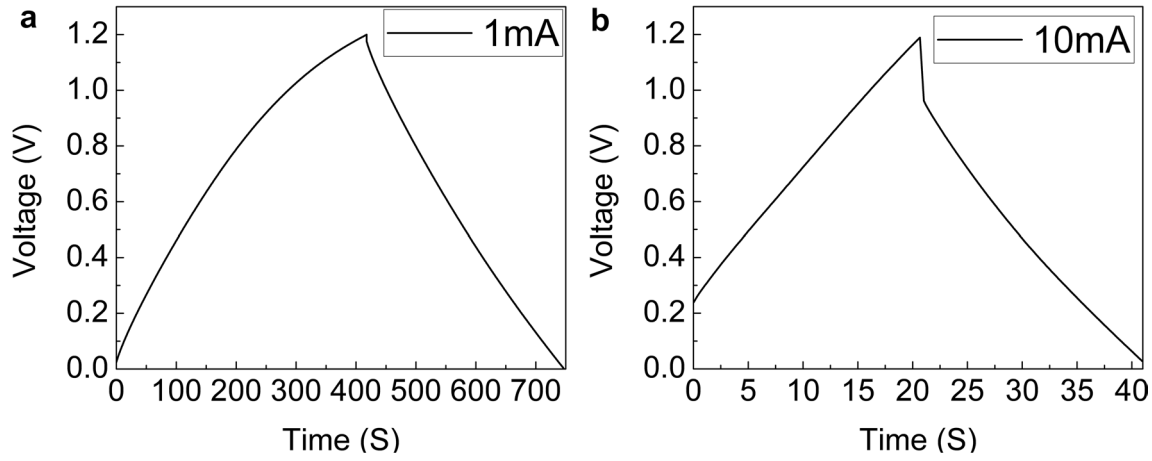

Fig. 6 Galvanostatic charge–discharge cycle with **a** 1 mA and **b** 10 mA for supercapacitor I

4 Conclusion

Monolithic supercapacitors have potential advantages for manufacturing and system integration, but have previously showed higher ESR and leakage current per capacitance [11] than laminated devices. A novel bio-derived composite materialmade from chitosan and MFC was used as a printable separator in monolithic aqueous supercapacitors and was found to improve the electrical performance of the devices to a level comparable with laminated supercapacitors. The ESR s is the same as measured for laminated components and the leakage current per capacitance is improved. The new material, CM5050, is easier to apply than chitosan and is thus advantageous from a manufacturing point of view. The correlation between leakage current and capacitance of the monolithic supercapacitors follows trends generally observed in supercapacitors. We also fabricated a supercapacitor in which both electrodes and current collectors were manufactured by screen printing to further enhance the possibility of potential industrial fabrication.

Acknowledgements The authors acknowledge the funding from the Academy of Finland (Grant Nos. 319041 and 326408). This work made use of Tampere Microscopy Center facilities at Tampere University. The infrastructure of Laboratory of Future Electronics at Tampere University is supported by Academy of Finland Finnish Research Infrastructure (FIRI, Grant No. 320019).

References

1. Somov A (n.d.) Powering IoT devices: technologies and opportunities—IEEE Internet of Things. https://iot.ieee.org/newsletter/november-2015/powering-iot-devices-technologies-and-opportunities.html. Accessed 22 May 2019
2. Roselli L, Mariotti C, Mezzanotte P, Alimenti F, Orecchini G, Virili M, Carvalho NB (2015) Review of the present technologies concurrently contributing to the implementation of the Internet of Things (IoT) paradigm: RFID, Green Electronics, WPT and Energy Harvesting. In: IEEE Topical Conference on Wireless Sensors and Sensor Networks (WiSNet), pp 1–3. https://doi.org/10.1109/WISNET.2015.7127402
3. Conway BE (1999) Electrochemical supercapacitors: scientific fundamentals and technological applications. Plenum Press, Berlin
4. Béguin F, Frąckowiak E (2013) Supercapacitors: materials, systems, and applications. Wiley, Hoboken
5. Kötz R, Carlen M (2000) Principles and applications of electrochemical capacitors. Electrochim Acta 45:2483–2498. https://doi.org/10.1016/S0013-4686(00)00354-6
6. Bagotskiĭ VS (2006) Fundamentals of electrochemistry. Wiley-Interscience, Hoboken
7. Keskinen J, Lehtimäki S, Dastpak A, Tuukkanen S, Flyktman T, Kraft T, Railanmaa A, Lupo D (2016) Architectural modifications for flexible supercapacitor performance optimization. Electron Mater Lett 12:795–803. https://doi.org/10.1007/s13391-016-6141-y
8. Tuukkanen S, Krebs M (2016) Printable power storage: batteries and supercapacitors. In: Giovanni Nisato SG, Lupo D (eds) Organic and printed electronics, 1st edn. Pan Stanford Publishing, New York, pp 265–291
9. Sagu JS, York N, Southee D, Wijayantha KGU (2015) Printed electrodes for flexible, light-weight solid-state supercapacitors—a feasibility study. Circuit World 41:80–86. https://doi.org/10.1108/CW-01-2015-0004

10. Zhan Y, Mei Y, Zheng L (2014) Materials capability and device performance in flexible electronics for the Internet of Things. J Mater Chem C 2:1220–1232. https://doi.org/10.1039/c3tc31765j
11. Keskinen J, Railanmaa A, Lupo D (2018) Monolithically prepared aqueous supercapacitors. J Energy Storage 16:243–249. https://doi.org/10.1016/J.EST.2018.02.008
12. Zu G, Shen J, Zou L, Wang F, Wang X, Zhang Y, Yao X (2016) Nanocellulose-derived highly porous carbon aerogels for supercapacitors. Carbon N Y 99:203–211. https://doi.org/10.1016/j.carbon.2015.11.079
13. Li Z, Liu J, Jiang K, Thundat T (2016) Carbonized nanocellulose sustainably boosts the performance of activated carbon in ionic liquid supercapacitors. Nano Energy 25:161–169. https://doi.org/10.1016/j.nanoen.2016.04.036
14. Jose J, Thomas V, Vinod V, Abraham R, Abraham S (2019) Nanocellulose based functional materials for supercapacitor applications. J Sci Adv Mater Dev 4:333–340. https://doi.org/10.1016/j.jsamd.2019.06.003
15. Du X, Zhang Z, Liu W, Deng Y (2017) Nanocellulose-based conductive materials and their emerging applications in energy devices - A review. Nano Energy 35:299–320. https://doi.org/10.1016/j.nanoen.2017.04.001
16. Chen W, Yu H, Lee SY, Wei T, Li J, Fan Z (2018) Nanocellulose: A promising nanomaterial for advanced electrochemical energy storage. Chem Soc Rev 47:2837–2872. https://doi.org/10.1039/c7cs00790f
17. Wang Z, Carlsson DO, Tammela P, Hua K, Zhang P, Nyholm L, Strømme M (2015) Surface modified nanocellulose fibers yield conducting polymer-based flexible supercapacitors with enhanced capacitances. ACS Nano 9:7563–7571. https://doi.org/10.1021/acsnano.5b02846
18. Lechêne BP, Cowell M, Pierre A, Evans JW, Wright PK, Arias AC (2016) Organic solar cells and fully printed super-capacitors optimized for indoor light energy harvesting. Nano Energy 26:631–640. https://doi.org/10.1016/j.nanoen.2016.06.017
19. Hu W, Zhong C, Deng Y, Qiao J, Zhang L, Zhang J (2015) A review of electrolyte materials and compositions for electrochemical supercapacitors. Chem Soc Rev 44:7484. https://doi.org/10.1039/c5cs00303b
20. Keskinen J (2018) Supercapacitors on flexible substrates for energy autonomous electronics. https://tutcris.tut.fi/portal/files/16507476/keskinen_1562.pdf. Accessed 22 May 22 2019
21. Tuukkanen S, Lehtimaki S, Jahangir F, Eskelinen A-P, Lupo D, Franssila S (2014) Printable and disposable supercapacitor from nanocellulose and carbon nanotubes. In: Proceedings of the 5th Electronics System-integration Technology Conference IEEE, pp. 1–6. https://doi.org/10.1109/ESTC.2014.6962740
22. Roy JC, Salaün F, Giraud S, Ferri A, Chen G, Guan J (2018) Solubility of chitin: solvents, solution behaviors and their related mechanisms. INTECH. https://doi.org/10.5772/intechopen.71385
23. Fiber Length of Pulp by Classification, Test Method T 233 cm-15, (n.d.) https://imisrise.tappi.org/TAPPI/Products/01/T/0104T233.aspx. Accessed 16 July 2019
24. Pettersson F, Keskinen J, Remonen T, von Hertzen L, Jansson E, Tappura K, Zhang Y, Wilén C-E, Österbacka R (2014) Printed environmentally friendly supercapacitors with ionic liquid electrolytes on paper. J Power Sources 271:298–304. https://doi.org/10.1016/J.JPOWSOUR.2014.08.020
25. Dighe AB, Dubal DP, Holze R (2014) Screen printed asymmetric supercapacitors based on $LiCoO_2$ and graphene oxide. Zeitschrift Für Anorg Und Allg Chemie 640:2852–2857. https://doi.org/10.1002/zaac.201400319
26. Jost K, Stenger D, Perez CR, Mcdonough JK, Lian K, Gogotsi Y, Dion G (2013) Knitted and screen printed carbon-fiber supercapacitors for applications in wearable electronics. Energy Environ Sci 6:2698–2705. https://doi.org/10.1039/c3ee40515j
27. Lehtimäki S (2017) Printed supercapacitors for energy harvesting applications. Tampere University of Technology. https://tutcris.tut.fi/portal/en/publications/printed-supercapacitors-for-energy-harvesting-applications(a7aeea33-1d5f-4f33-8dbc-437cc81a9cbe)/export.html
28. Barsoukov E, Macdonald JR (2005) Impedance spectroscopy: theory, experiment, and applications. Wiley, Hoboken
29. IEC 62391-1:2015 | IEC Webstore (n.d.) https://webstore.iec.ch/publication/23581. Accessed 22 May 2019
30. Lehtimäki S, Railanmaa A, Keskinen J, Kujala M, Tuukkanen S, Lupo D (2017) Performance, stability and operation voltage optimization of screen-printed aqueous supercapacitors. Sci Rep 7:1–9. https://doi.org/10.1038/srep46001